Extended carbonyl-rich conjugated polymer cathode for high capacity lithium-ion batteries

Shibing Zheng[a], Licheng Miao[b], Tianjiang Sun[a], Lin Li[a], Tao Ma[a], Junquan Bao[a], Zhanliang Tao*[a] Jun Chen[a]

[a] *Key Laboratory of Advanced Energy Materials Chemistry (Ministry of Education), College of Chemistry, Nankai University, Tianjin 300071, China.*

[b] *College of Physics and Optoelectronic Engineering, Shenzhen University, Shenzhen 518060, China.*

**Corresponding author (E-mail: taozhl@nankai.edu.cn)*

Experimental Section

All reagents were purchased from commercial sources without further purification, anaerobic water and tetrahydrofuran (THF) were prepared by flash freezing the glass ampule in a liquid nitrogen bath, and thawing with an internal pressure < 20 mbar, then transfer them into the glovebox after three freeze/unfreeze cycles.

Synthesis of the PTO-Br_2

In a 100 mL Schlenk-flask, 600 mg (2.28 mmol) of pyrene-4,5,9,10-tetraone was added into H_2SO_4 (15 mL) and then 900 mg (5.1 mmol) of N-bromosuccinimide (NBS) was added into the mixture in batches. The resulting mixture was stirred at 45 ^oC for 2 h. A yellow precipitate was obtained by dropping the reaction mixture into the ice water (500 mL, 0-5 ^oC) and was collected by filtration. The residue was purified by recrystallization from dimethyl sulfoxide (DMSO) and wash with ether and dichloromethane to yield the desired product (0.63 g, 66%). ^{1}H-NMR (DMSO-$_{d6}$, 500 MHz): δ = 8.36 (s, 4H).[1]

Synthesis of the PPh-PTO

84 mg (0.4 mmol) of benzene-1,3,5-triyltriboronic acid (BTA, Extension), 252.2 mg (0.6 mmol) of 2,7-dibromo-4,5,9,10-pyrenetetrone (PTO-Br_2) and 663 mg (4.8 mmol) of potassium carbonate (K_2CO_3) were add into a 80 ml teflon reactor, then in the glovebox filled with Ar atmosphere (H_2O ＜ 0.1, O_2 < 0.1 ppm), 70 mg (0.06 mmol) tetrakis(triphenylphosphine)palladium ($Pd(PPh_3)_4$) and

24 mL tetrahydrofuran / water (v, 1:1) were added, placed the sealed reactor in an oven at 135 ^{o}C and left undisturbed for 72 h, washed with water/tetrahydrofuran and stirred at 10% nitric acid at 60 ^{o}C for 24 h (to dissolve the palladium black). Subsequently Soxhlet extraction with tetrahydrofuran for 24 h, then dried on 80 ^{o}C in vacuum for 12 h to obtain the as-prepared PPh-PTO, and the sample was finally annealed at 150 °C for 12 h under argon atmosphere to yield the annealed-PPh-PTO a black powder (156 mg, 81% yield). And the following tests were all based on the annealed-PPh-PTO.

Material characterizations:

Proton magnetic resonances (^{1}H NMR) were conducted on Bruker Avance III 400MHz. Solid-state cross polarization magic angle spinning nuclear magnetic resonance (CPMAS-NMR) were collected on Agilent 600MHz.Transform Infrared Spectroscopy (FTIR) was recorded with Bruker 46 TENSOR II. UV-Vis absorption spectra were collected on SPEC ORD 2010 plus Analytikjena. Raman spectrum was gathered through confocal microscope Horiba LabRAM HR Evolution (excitation wavelength of 633 nm). Thermal gravimetric analysis (TGA) was carried out with NETZSCH STA449F3 in Ar atmosphere. X-ray diffraction (XRD) tests were performed on Rigaku MiniFlex 600 with Cu Kα radiation. The contact angles were obtained on Physics OCA 25. Brunauer-Emmett-Teller (BET) and the pore size distribution was analyzed using the Barrett-Joyner-Halenda (BJH) model. X-ray photoelectron spectroscopy (XPS) characterization was conducted on PHI5000Versa Probe ESCALAB 250xi. The microstructure and morphology were observed by field-emission scanning electron microscopy (SEM, JEOL JSM7500F) and high-resolution transmission electron microscopy (HRTEM, Talos F200X G2) equipped with energy dispersive spectroscopy (EDS) for elemental analysis. Contact angles were conducted by using a contact angle measurement (Data physics, TBU 100).

Electrode Preparation and Measurements:

The PPh-PTO based electrodes for the general tests and ex-situ XPS were prepared by grinding the 60 wt% treated PPh-PTO, 30 wt% Ketjenblack ECP600JD (KB) (Lion Coporation), 10 wt% polyvinylidene fluoride (PVDF) (Sinopharm Chemical Reagent Co., Ltd.) and drops of N-methyl-2-pyrrolidinone (NMP) (Alfa Aesar, ≥ 99%), then coating the slurry on clean aluminum foil. After drying in vacuum (80 ^{o}C, 12 h), the electrodes loading with around 1 mg cm^{-2} of PPh-PTO were

achieved. Subsequently, CR-2032 coin cell batteries were assembled with the prepared electrode as the cathode and polished lithium as the counter electrode, then 40 μL of 1 M lithium perchlorate ($LiClO_4$) in tetraethylene glycol dimethyl ether (G4) was employed as the electrolyte. The electrochemical performance of PPh-PTO was evaluated by galvanostatic charge/discharge (GCD) on LAND CT2001A, and cyclic voltammetry (CV) curves were collected by the electrochemical workstation (CHI 660E) within a potential 1.5 - 3.8 V.

The electrodes for the in-situ FTIR and ex-situ Raman test were prepared by grinding PPh-PTO, KB and PTFE (10 wt% PTFE dispersion in water) in a weight ratio of 7:2:1. Then the slurry was cast on the stainless steel net collector. After dried at 80 °C for 12 h under vacuum, the coin-type cell with a detection window was assembled in the Ar-filled glove box. The assembled cells for in-situ FTIR measurements were cycled at a current density of 0.25 A g^{-1} in the range of 1.5 - 3.8 V.

Supporting Figures, Discussions

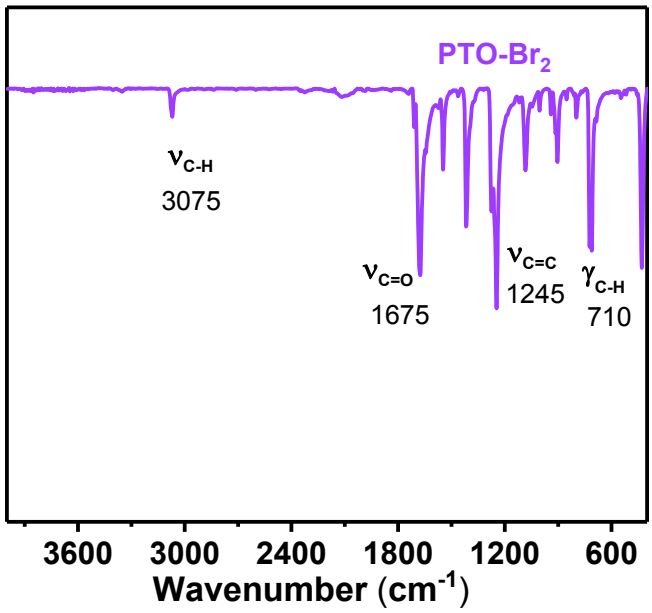

Figure S1. FTIR spectrum of PTO-Br_2

The peak at 3075 cm^{-1} is the stretching vibration of -C-H, 1675 cm^{-1} is the stretching vibration of -C=O, 1245 cm^{-1} is the stretching vibration of the aromatic ring and 710 cm^{-1} is the in-plane bending vibration of -C-H.

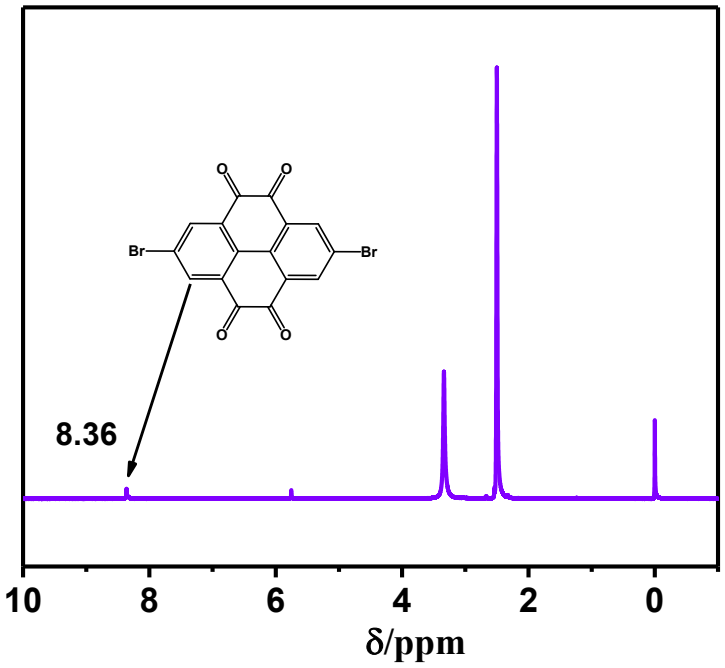

Figure S2. ^{1}H NMR (400 MHz, DMSO-d_6, 298 K) spectrum of PTO-Br_2.

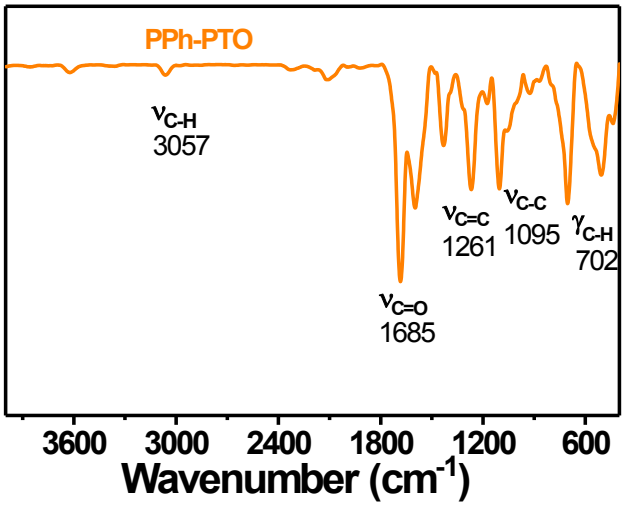

Figure S3 FTIR spectrum of PPh-PTO.The peak at 3057 cm^{-1} is the stretching vibration of -C-H, 1685 cm^{-1} is the stretching vibration of -C=O, 1261 cm^{-1} is the stretching vibration of the aromatic ring, 1095 cm^{-1} is the stretching vibration of -C-C and 702 cm^{-1} is the in-plane bending vibration of -C-H.

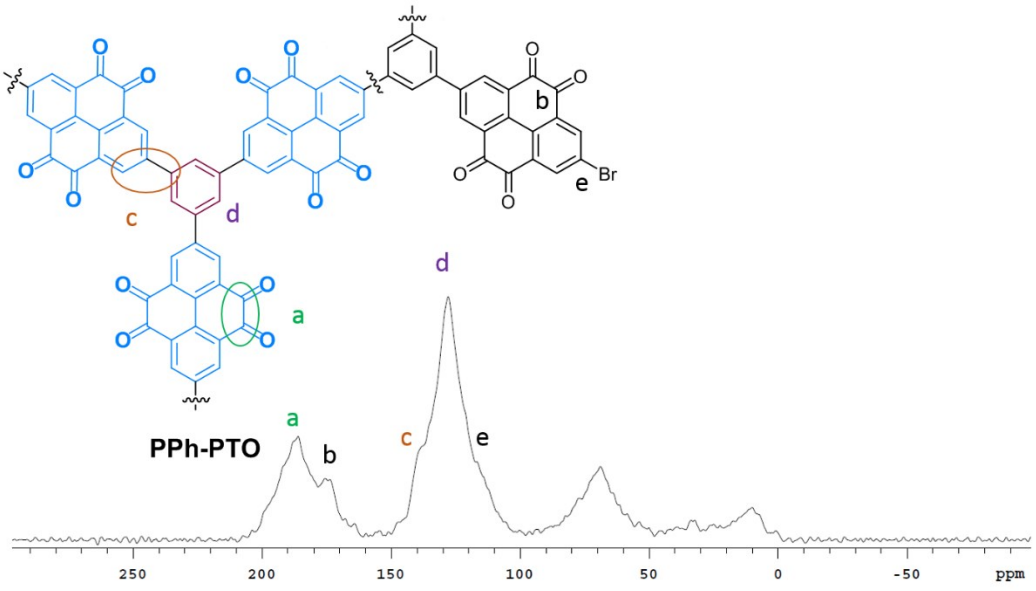

Figure S4. Solid-state ^{13}C NMR (600MHz) spectrum of PPh-PTO, and the peaks at 70 and 10 ppm are the C-P bond at the tail end formed during the suzuki reaction.

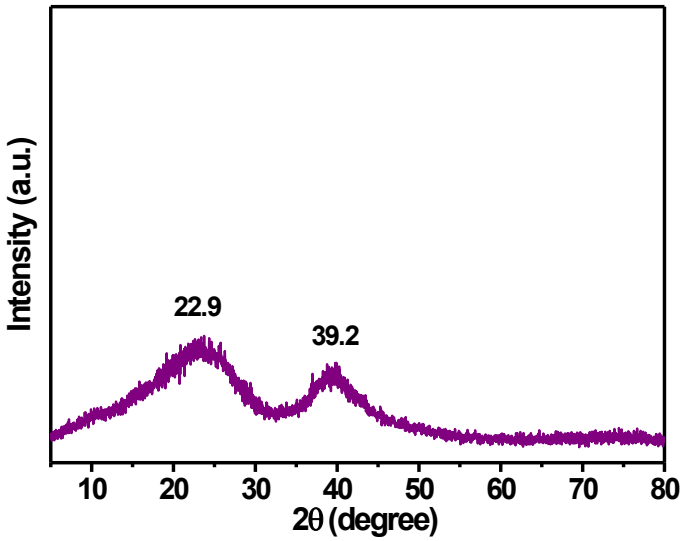

Figure S5 XRD pattern of PPh-PTO.

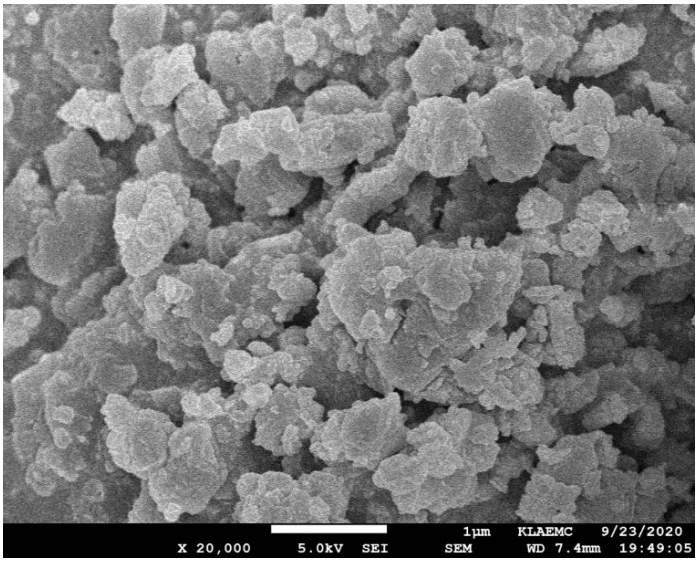

Figure S6. SEM image of PPh-PTO.

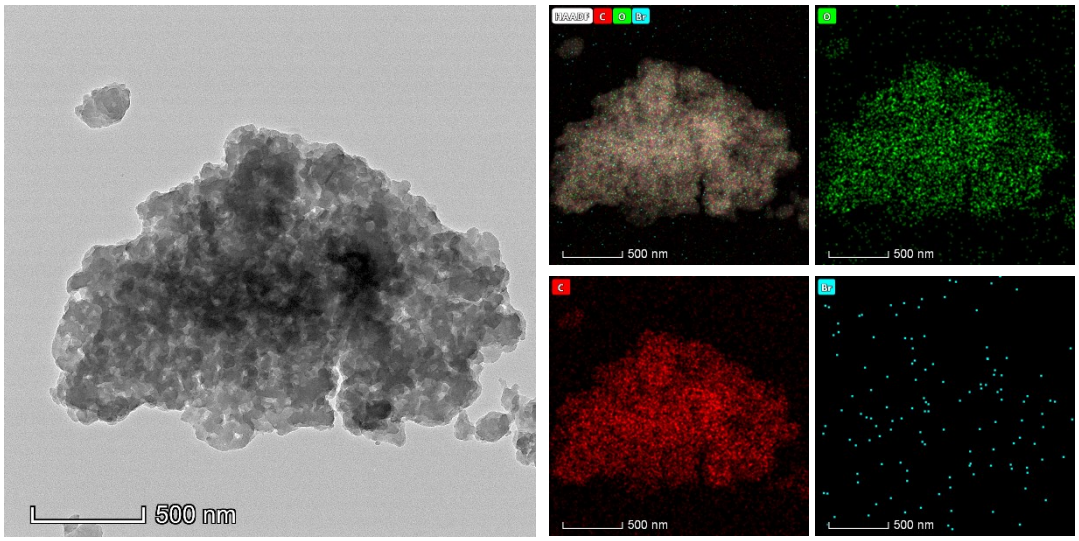

Figure S7. HRTEM image of PPh-PTO and corresponding element mapping.

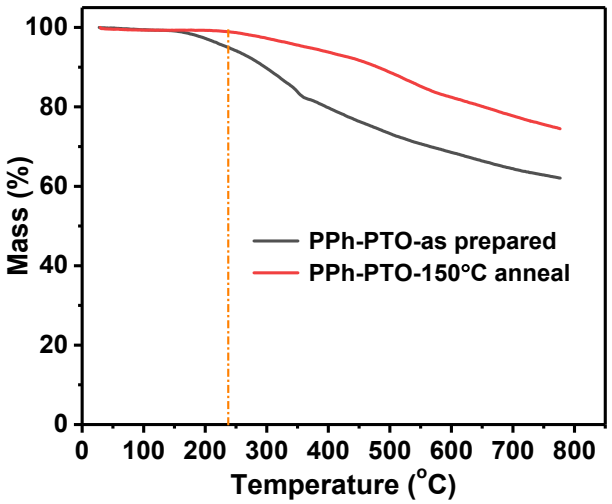

Figure S8. TG curves of the as-prepared (black) PPh-PTO (dried in vacuum before the test) and anneal-treated (red) sample at Ar atmosphere, and the remarkable weight loss between 250 - 770 °C can be ascribed to the decomposition of PPh-PTO skeleton.

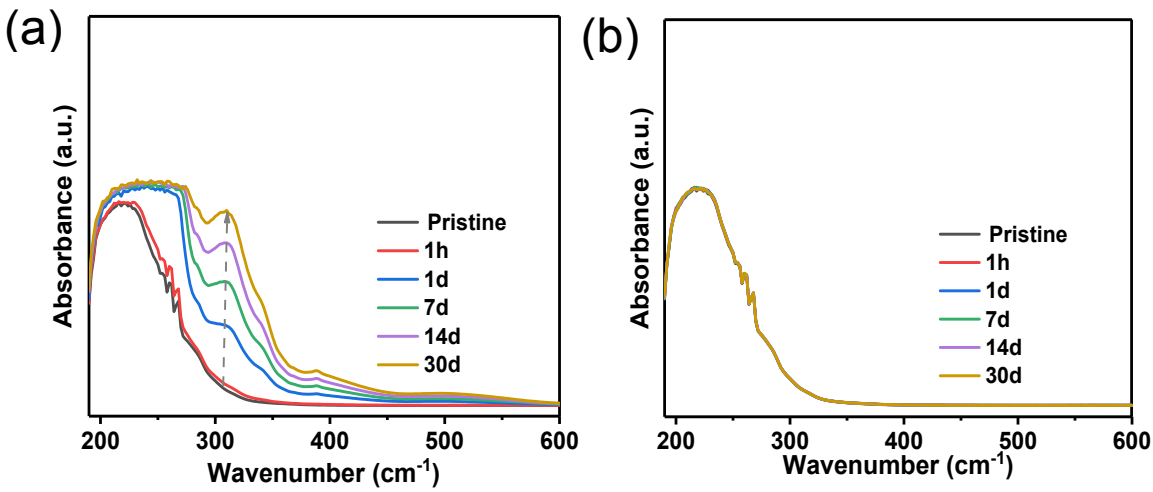

Figure S9. Ex-situ Uv-vis spectra of the electrolyte after soaking different time for (a) PTO electrode (b) PPh-PTO electrode.

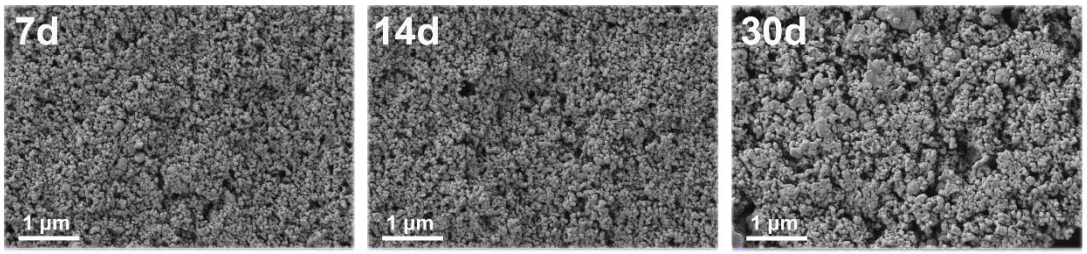

Figure S10. The morphologies of the pristine and soaked (7, 14, 30 days) PPh-PTO electrodes.

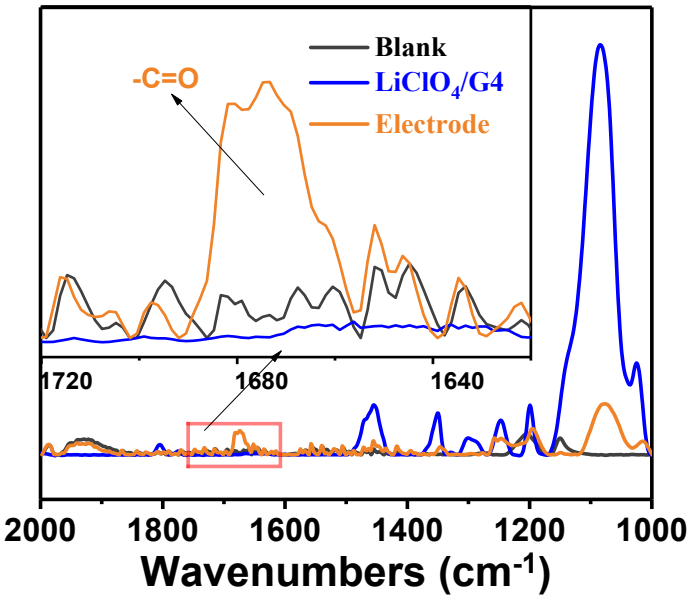

Figure S11. The FTIR absorbance curves of the blank electrode, $LiClO_4$/G4 electrolyte

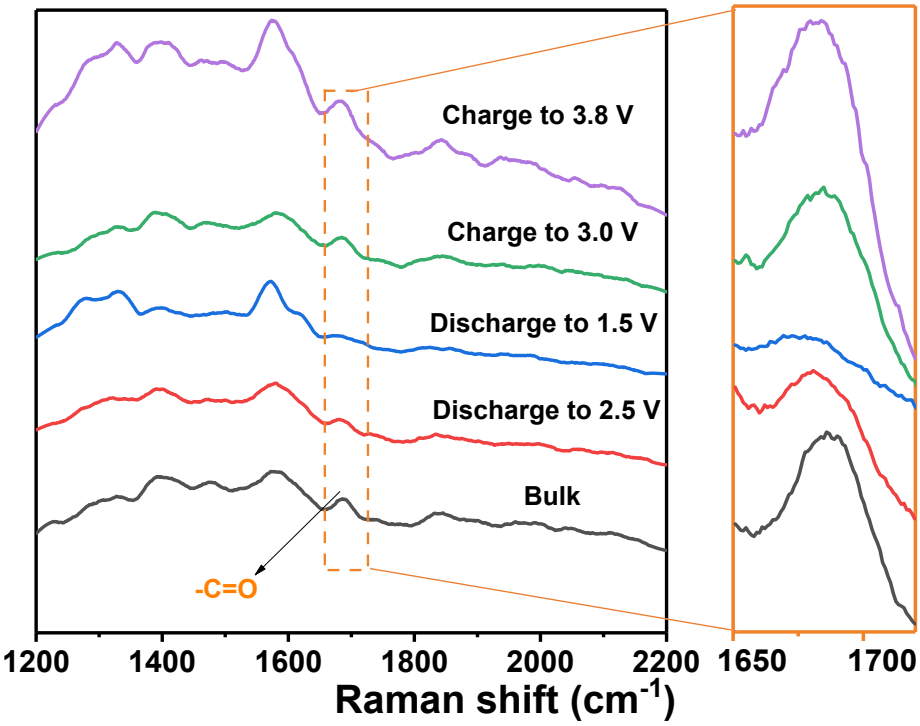

and the PPh-PTO electrode.

Figure S12. Ex-situ Raman spectra of PPh-PTO at different discharge-charge states.

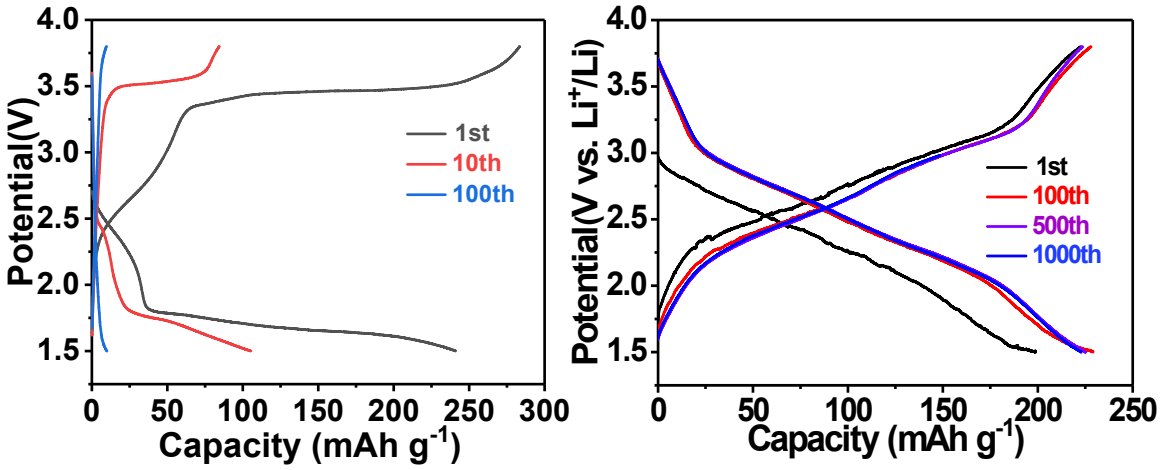

Figure S13. The discharge/charge curves of PPh-PTO in 1 M LiTFSI + DOL/DME (v/v: 1/1) (a) and 1M $LiClO_4$/G4 (b) at the current density 0.1 A g^{-1}.

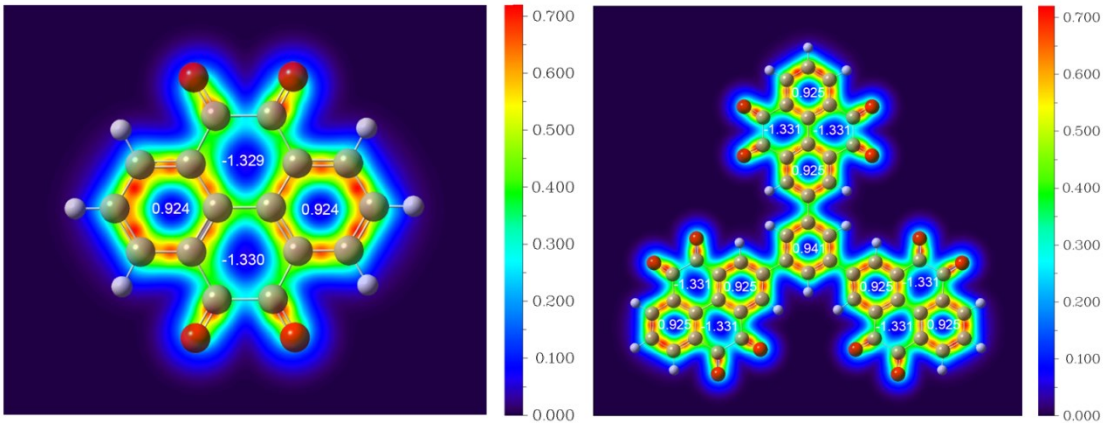

Figure S14. The LOL-π and HOMA calculation of every six-membered ring in PTO (left) and PPh-PTO (right). LOL-π[2] and HOMA[3] are the ways to measure the aromaticity of planar organic molecules, in which LOL-π is a three-dimensional function to qualitatively illustrate the delocalization of π electrons and HOMA is a quantitative method to reflect the aromaticity of every part of a molecule. Note that the stronger aromaticity of the studied molecule is close to 1. If HOMA is close to 0, the molecule will be non-aromatic. If the value is negative, the bond length will be extremely uneven, reflecting anti-aromaticity characteristics of the molecule. As shown on the LOL-π in the Figure S14, compared with the PTO, the PPh-PTO has more 6-

membered aromatic rings (the red cycle). In addition, every 6-membered aromatic ring of PPh-PTO has a higher HOMA value than that of PTO, indicating that aromaticity of the PPh-PTO is stronger.

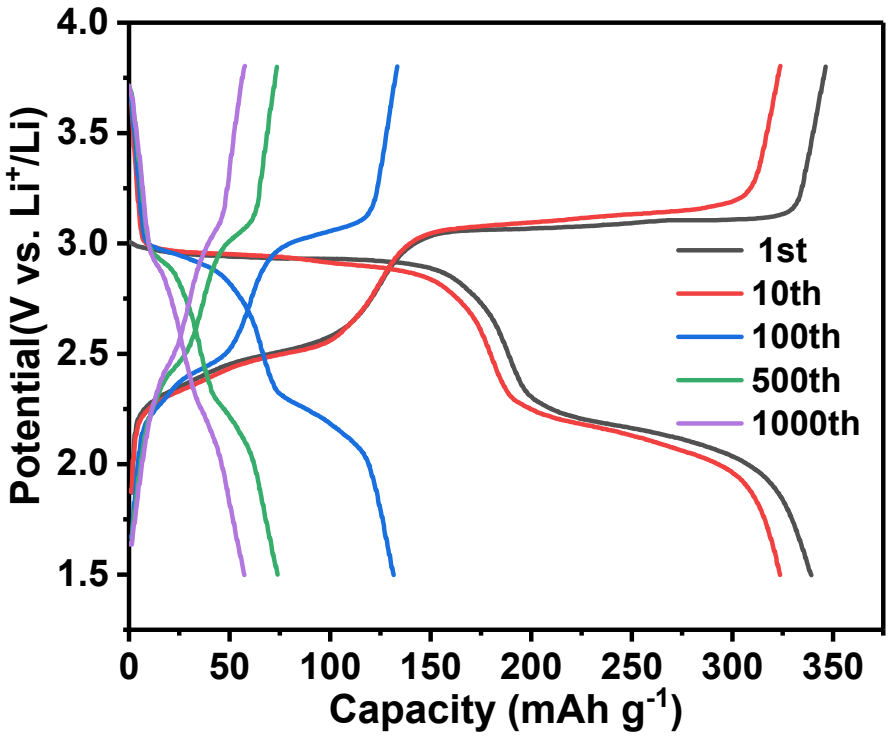

Figure S15. The discharge/charge curves of PTO at different cycles with the current density 0.1 A g^{-1}.

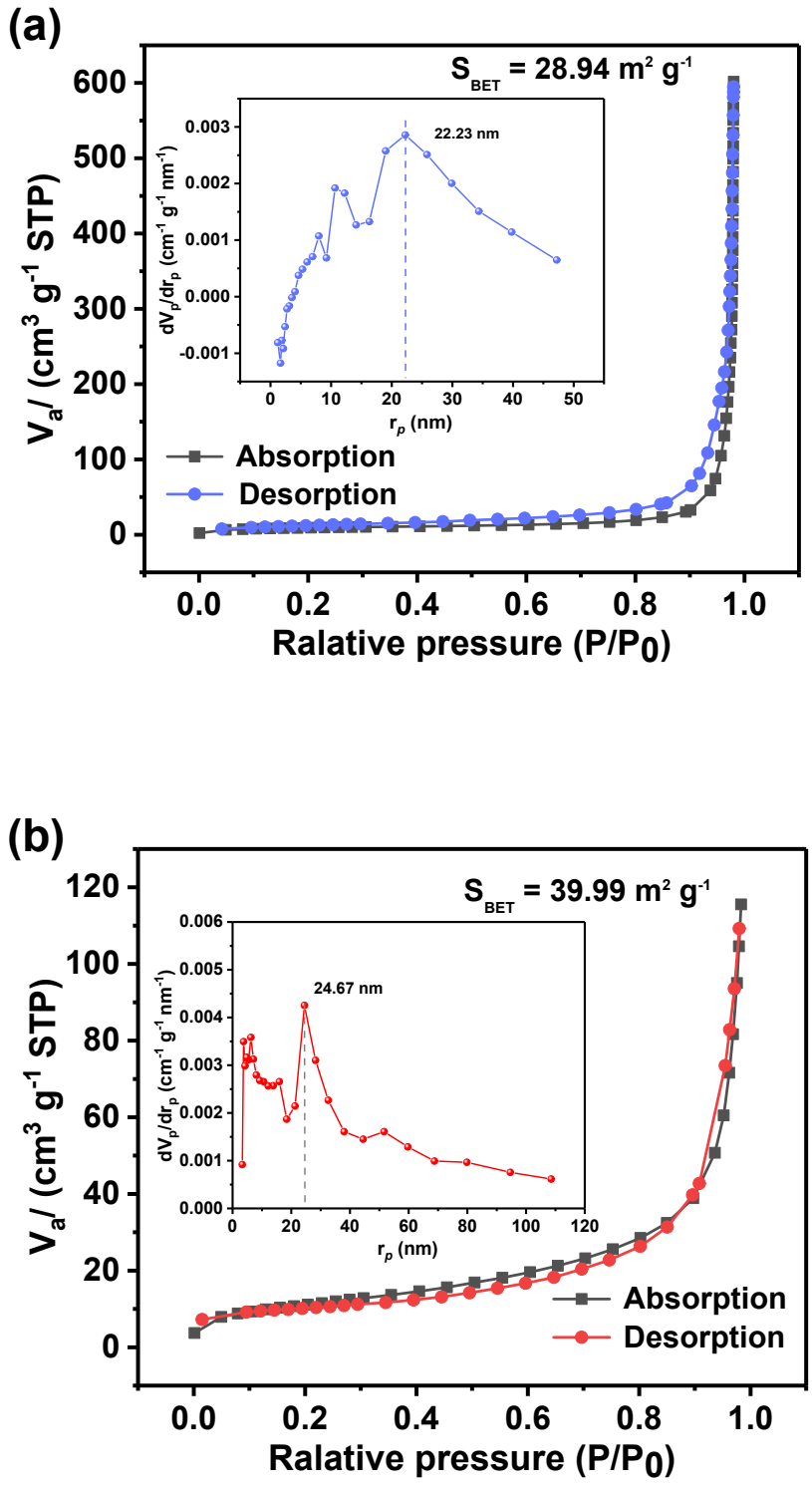

Figure S16 N_2 adsorption/desorption isotherms of the origin (a) and annealed (b) PPh-PTO. The inset is the corresponding pore size distributions.

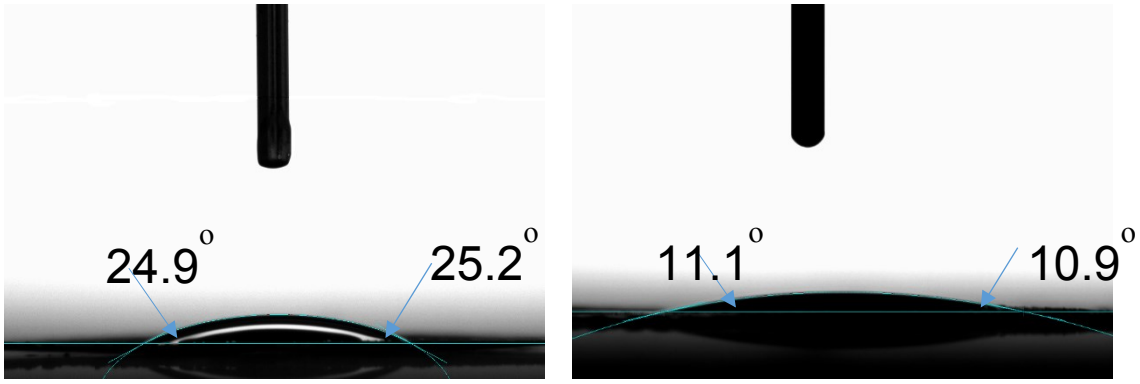

Figure S17 Contact angle for the electrolyte of 1.0 M $LiClO_4$/G4 with PTO (left) and PPh-PTO (right) electrode plate. The electrode could be wetted in 1 s, and the PPh-PTO cathode showed better compatibility with the electrolyte than PTO cathode.

Computational details

Density functional theory (DFT) calculations were performed with Gaussian 16 software package.[4] The geometries were fully optimized for each molecule at the B3LYP/6-31+G (d, p). The HOMO and LUMO plots were obtained by using GaussView 6. LOL-π and HOMA calculations were performed by Multiwfn 3.7.[5] All visualization of MESP plots were performed by Visual Molecule Dynamics (VMD) software.

Reference:

[1] S. Kawano, M. Baumgarten, D. Chercka, V. Enkelmann, K. Mullen, *Chem. Commun.* 2013, **49**, 5058-5060.

[2] a) H. Schmider, A. Becke, *J. Mol. Struct*. 2000. 527, 51-56; b) S. N. Steinmann, Y. Mo, C. Corminboeuf, *Phys. Chem. Chem. Phys.* 2011, **13**, 20584-20592.

[3] L. Miao, L. Liu, K. Zhang, J. Chen, *ChemSusChem* 2020, **13**, 2337-2344.

[4] M. Frisch, G. Trucks, H. Schlegel, G. Scuseria, M. Robb, J. Cheeseman, G. Scalmani, V. Barone, B. Mennucci, G. Petersson, et al. Gaussian 16, Revision A.03; Gaussian, Inc.: Wallingford, CT, 2016.

[5] T. Lu, F. Chen, *J. Comput. Chem.* 2012, **33**, 580-592.